Sensitivity Analysis of a Cardio-respiratory Model for Pulse Transit Time

Arthur Ben-Tolila[1], Virginie Le Rolle[1], Alfredo I. Hernández[1]

[1] Univ Rennes, Inserm, LTSI - UMR 1099, F-35000 Rennes, France

Abstract

The pulse transit time (PTT) is the pulse pressure delay typically computed between the ECG R wave and the pulse arrival at the periphery. While this non-invasive biomarker correlates with various physiological parameters, the mechanisms modulating it remain poorly understood. This study investigates the influence of the cardio-respiratory system (CRS) on PTT, using knowledge-based modeling. A previously developed model of the CRS was enriched with a finger compartment, and the PTT was computed as the time between the left ventricle activation and the arrival of the pulse pressure wave in the finger capillaries. A Morris sensitivity analysis was performed on model parameters. The most influential on the mean PTT were parameters defining the ventricular elastance, the extrathoracic arteries, and the finger vessels. PTT oscillations were also influenced by respiratory parameters. These results highlight a convenient set of parameters to be identified for subject-specific modeling.

1. Introduction

The pulse transit time (PTT) refers to the time that a blood pressure wave takes to travel from one arterial site to another. While many types of PTT have been studied, it is typically computed as the delay between the left ventricular ejection time, approximated by the ECG R-wave, and the arrival of the pulse at a peripheral site, derived from a photoplethysmography (PPG) signal recorded at the finger, ear or toe [1–3].

PTT can be acquired non-invasively, continuously, and in a portable manner [1, 3], and has been shown to correlate with a variety of physiological variables, including arterial stiffness [2], blood pressure (BP) [2, 3], and respiratory effort [4]. This explains the interest in this signal for applications such as continuous blood pressure estimation [2, 3] and sleep apnea monitoring [1, 4, 5]. Yet despite this interest, the physiological origins of the PTT and PPG signals are still not fully understood. For instance, although researchers agree that PTT is negatively correlated with systolic BP, correlation coefficients vary greatly between studies, measurement sites, and individuals, suggesting the involvement of multiple and interconnected physiological phenomena [3].

In this context, a model-based approach is well-suited for investigating the influence of cardio-respiratory interactions on PPG and PTT signals, by directly integrating knowledge concerning these physiological systems. Several models have been proposed for the analysis of PPG signals. Charlton et al. [6] simulated pulse waves and PPG using a 1-D arterial network and studied pulse wave velocities, but did not include a heart model, respiratory interactions or gas transport. While not producing PPG signals specifically, Broomé et al. [7] synthesized blood pressure waves in detailed vascular compartments using a closed-loop lumped-parameter model of the heart, valves, circulation, oxygen transport and neural interactions, but did not use a respiratory model or study PTT. Beside knowledge-based models, other works focused on synthetizing a PPG signal from patient data, such as that of Sološenko et al. [8]; but they did not integrate respiratory modulation of the PPG, or aim to synthetize PTT. To our knowledge, no existing model from the literature integrates all cardiac, circulatory, respiratory and PPG submodels, for the analysis of PTT signals.

Our team has recently proposed an complete integrated model of cardio-respiratory interactions [9, 10]. However, this model should be adapted to simulate a pulse wave to the finger in order to synthesize a PPG signal and the associated PTT. The objectives of this work are : 1) to propose an integrated cardio-respiratory model to synthesize a PTT signal, 2) to analyze the effects of the most relevant parameters of the proposed model on PTT characteristics by applying a sensitivity analysis method.

2. Methods

2.1. Model description

The closed-loop cardio-respiratory model presented in this study (fig. 1) is derived from previous work by our team [9, 10], and integrates three connected submodels: i) the cardiovascular system, ii) the respiratory system, iii) the gas exchange system. Previous work also includes a neural control submodel, with chemoreflex and baroreflex

loops. However, they were turned off in this study in order to focus on cardiovascular and respiratory effects. Furthermore, a new finger compartment was added to represent the PPG measurement site, as the finger is the most common measurement point in the literature [1, 2, 4, 5].

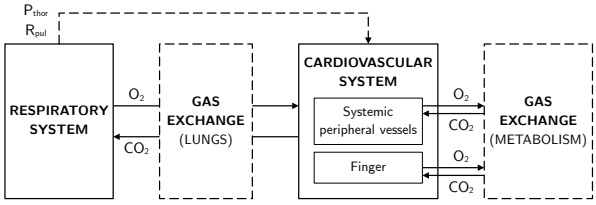

Figure 1. Cardio-respiratory model diagram. Dotted line arrows symbolyze interactions between submodels. P_{thor}, thoracic pressure; R_{pul}, pulmonary capillaries resistance.

2.1.1. Cardiovascular system model

The cardiovascular system model (fig. 2) consists of a cardiac electrical activity model, a cardiac mechanical activity model, and a circulation model [9]. The cardiac electrical activity relies on interconnected automata representing groups of cardiac cells [11]. They trigger the ventricular and atrial activations in the cardiac mechanical activity model, which is based on elastances [12, 13]. Notably, the elastance $e_v(t)$ for both ventricles ($v \in \{lv, rv\}$) is defined by a Two-hill driving function:

$$e_v(t) = C \cdot \left(\frac{\left(\frac{t}{\alpha_1 T}\right)^{n_1}}{1 + \left(\frac{t}{\alpha_1 T}\right)^{n_1}} \right) \cdot \left(\frac{1}{1 + \left(\frac{t}{\alpha_2 T}\right)^{n_2}} \right) \quad (1)$$

where C is a positive constant, T is the heart period, and n_1, n_2, α_1 and α_2 are model parameters [9]. Ventricular blood pressure is then computed as:

$$P_v(V_v, t) = e_v(t) \cdot P_{es}(V_v) + (1 - e_v(t)) \cdot P_{ed}(V_v) + P_{thor} \quad (2)$$

where P_{es} and P_{ed} are the end-systolic and end-diastolic pressures, respectively:

$$P_{es}(V_v) = E_{v,es} \cdot (V_v - V_{uv}) \quad (3)$$

$$P_{ed}(V_v) = P_0 \cdot (e^{\lambda \cdot (V_v - V_0)} - 1) \quad (4)$$

Finally, the end-systolic ventricular elastance $E_{v,es}$ is defined with two parameters, $E_{v,MIN}$ and $E_{v,MAX}$:

$$E_{v,es} = E_{v,MIN} + \frac{E_{v,MAX} - E_{v,MIN}}{2} \quad (5)$$

The circulation model (fig. 2) integrates the systemic and pulmonary circulations. Vascular compartments are defined by their unstressed volume and elastance E, and connected by resistances R, as well as inductances L for arterial compartments [9]. The finger circulation, integrating arterial, capillary and venous subcompartments, has been placed in parallel to the systemic peripheral vessels compartment, representing the rest of the peripheral circulation. The pressure in the finger capillary compartment is denoted P_F.

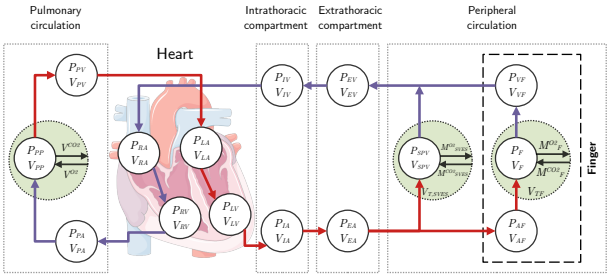

Figure 2. Circulatory model diagram. Compartments with a green area are involved in gas exchange. Each vascular compartment has pressure and volume states. Acronyms: LA/LV: left atrium and ventricle, RA/RV: right atrium and ventricle, $PA/PP/PV$: pulmonary artery, vessels and vein, IA/IV: intrathoracic arteries and veins, EA/EV: extrathoracic arteries and veins, SPV: systemic peripheral vessels, $AF/F/VF$: finger arteries, capillaries and veins.

2.1.2. Respiratory model

The respiratory model comprises the airways (upper, intermediate, lower), the alveolar compartment, the pleural cavity, the chest wall, and the respiratory muscles [14].

2.1.3. Gas exchange model

The gas exchange model was defined in [9, 10] and comprises gas exchange in the lungs and the metabolism, and gas transport through the blood circulation. Both the systemic peripheral vessels compartment and the finger capillary compartment consume O_2 and produce CO_2.

2.2. Pulse transit time modeling

It was hypothesized that the blood pressure signal in the finger capillary compartment (denoted P_F) could be interpreted as a PPG signal. For each beat i, one PTT_i value was calculated by measuring the time between the left ventricular activation from the corresponding cellular automata, and the start of the corresponding pulse on P_F, computed using the intersecting tangents method [2] (fig. 3). The mean PTT value ($\overline{PTT}$) over a simulation period containing N_h heartbeats is :

$$\overline{PTT} = \frac{1}{N_h} \sum_{i \leq N_h} PTT_i \quad (6)$$

The modulation of the PTT signal by respiration [1, 4] was evaluated by quantifying the amplitude of its oscillations. A local maxima M_j and minima m_j detection was first performed to calculate $\Delta PTT_j = M_j - m_j$ for each

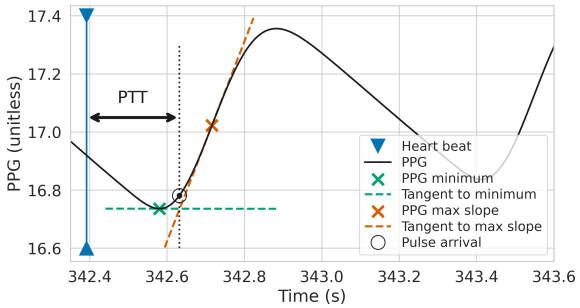

Figure 3. PTT computation using the intersecting tangents method [2].

respiratory cycle j (fig. 4). The average value $\overline{\Delta PTT}$ over a simulation period containing N_r respiratory cycles was calculated as:

$$\overline{\Delta PTT} = \frac{1}{N_r} \sum_{j \leq N_r} \Delta PTT_j \tag{7}$$

2.3. Sensitivity analysis

A Morris's sensitivity analysis [15] was applied to establish a rank of importance between model parameters $(X_1, ..., X_k)$ based on their influence on PTT. This method explores a predefined range of the parameter space by dividing it into a regular grid of p levels, choosing a random starting point $(x_1, ..., x_k)$ on this grid, and varying each parameter in turn on this grid by Δ, generating an elementary effect EE_i for each of them:

$$EE_i = \frac{F(x_1, ..., x_i + \Delta, ..., x_k) - F(x_1, ..., x_i, ..., x_k)}{\Delta} \tag{8}$$

where F is a function of the model output variables (the output function). This method can be repeated r times to obtain r elementary effects. For each parameter X_i, the mean of the absolute values μ_i^*, the standard deviation σ_i, and the Morris distance $D_i = \sqrt{(\mu_i^*)^2 + (\sigma_i)^2}$ of the r elementary effects are computed to evaluate the importance of each parameter.

In this study, each of the 112 model parameters was evaluated in a range of $\pm 30\%$ of their initial value, with $p = 20$ and $r = 100$. The two output functions ($\overline{PTT}$ and $\overline{\Delta PTT}$) were calculated over 120 seconds of simulation, after a stabilization period of 300 seconds.

3. Results and discussion

3.1. Model output

Figure 4 shows the modeled lung volume, intrathoracic arterial pressure P_{IA}, finger capillary pressure P_F, and pulse transit time, on a 15 second extract of this period. The average systolic and diastolic P_{IA} are 115 and 78 mmHg respectively, and the mean P_F is 17 mmHg [16]. P_F and the PTT appear clearly modulated by respiration [4]. The mean pulse transit time $\overline{PTT}$ is 242.38 ms [2], and the mean PTT oscillation $\overline{\Delta PTT}$ is 7.41 ms [4, 5].

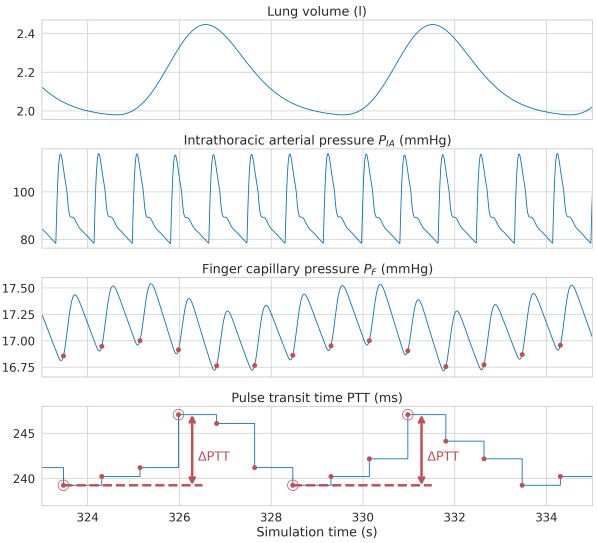

Figure 4. Simulation output after stabilization. The red dots show the pulse arrivals computed using the intersecting tangents method.

3.2. Morris sensivity analysis results

Figure 5 shows the results of the Morris sensitivity analysis for $\overline{PTT}$ (a) and $\overline{\Delta PTT}$ (b). Parameters are sorted by Morris distance D_i, and only the 15 most influent are displayed for each output function.

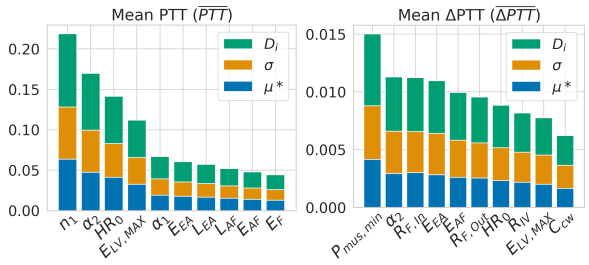

Figure 5. Morris sensitivity analysis results for (a) mean PTT, (b) mean ΔPTT. See fig. 2 for the signification of indices.

The most sensitive parameters are related to the following physiological mechanisms:

Ventricular elastance parameters n_1, α_1, α_2 (eq. 1) directly modify the shape of the ventricular elastance function. Increasing one of these parameters reduces the initial upwards slope of the left ventricular pressure P_{LV}, delaying the ejection of blood and increasing $\overline{PTT}$. A decrease in maximum LV contractility $E_{lv,max}$ (eq. 5) has the same effect. This is coherent with the findings of Villegas-Martinez et al. [17] who found an increase in PTT in left bundle branch block, where the left ventricular pressure rise is slowed down.

Extrathoracic circulation parameters (elastance E_{EA} and inductance L_{EA}) and **finger vascular parameters** for the arterial (elastance E_{AF} and inductance L_{AF}) and capillary (elastance E_F, inflow and outflow resistances $R_{F,In}$ and $R_{F,Out}$) compartments are mainly involved in the velocity of the pulse pressure wave. Pulse waves travel faster in stiffer vessels (larger E) and slower with more vascular resistance (larger R), which is coherent with what has been demonstrated in vivo [2,16] and in silico [6]. Furthermore, compliant (smaller E) and more resistant (larger R) vessels dampen the systolic pulse waves, but amplify vasomotor movement due to respiration which creates higher $\overline{\Delta PTT}$. Greater inertia of the blood flow (L) deccelerates the transmission of the upwards pressure slope to downstream compartments, and therefore increases $\overline{PTT}$.

Systemic peripheral vessels (SPV) inflow and outflow resistances $R_{SPV,In}$ and $R_{SPV,Out}$ control the flow of blood into the finger vessels, which are in parallel with the SPV (see fig. 2). Higher R_{SPV} values increase P_{AF} but flatten it, thus delaying the time of its maximum slope, which feeds back into P_F and results in prolonged PTT.

Respiratory parameters influence $\overline{\Delta PTT}$ indirectly: the minimum respiratory muscles pressure $P_{mus,min}$ and the chest wall compliance C_{cw}. Inspiration slightly reduces systolic BP, thus the amplitude of the BP signal is modulated at the respiratory frequency. In the circulatory model, all pressures are affected, starting from P_{IA}, and notably P_F where PTT is computed. Greater respiratory effort, involved by higher C_{cw} or lower (negative) $P_{mus,min}$, therefore produces larger swings in PTT with each respiratory cycle. This effect is visible on real PPG and PTT signals and has been exploited in the literature to detect and characterize apneas [4, 5].

Heart rate parameter HR_0 sets the heart rate of the model, since neural control of the heart rythm is turned off. A slower heart rate gives more time for the chambers to fill with blood, increasing contractility through the Frank-Starling mechanism; this results in a larger slope of P_{LV} and therefore a smaller $\overline{PTT}$.

4. Conclusion

This study presents a model-oriented approach to understanding PTT dynamics, using an integrated model of cardio-respiratory interactions. A set of model parameters was identified as influential on the mean PTT and the mean PTT oscillation, which will allow for patient-specific identification in future works.

References

[1] Smith R, et al. Pulse transit time: an appraisal of potential clinical applications. Thorax 1999;54(5):452–457.

[2] Finnegan E, et al. Pulse arrival time as a surrogate of blood pressure. Sci Rep 2021;11(1):22767.

[3] Ding X, Zhang YT. Pulse transit time technique for cuffless unobtrusive blood pressure measurement: from theory to algorithm. Biomed Eng Lett 2019;9(1):37–52.

[4] Pitson D, et al. Use of pulse transit time as a measure of inspiratory effort in patients with obstructive sleep apnoea. Eur Respir J 1995;8(10):1669–1674.

[5] Pagani J, et al. Detection of central and obstructive sleep apnea in children using pulse transit time. In Computers in Cardiology, volume 29. 2002; 529–532.

[6] Charlton PH, et al. Modeling arterial pulse waves in healthy aging: a database for in silico evaluation of hemodynamics and pulse wave indexes. Am J Physiol Heart Circ Physiol 2019;317(5):H1062–H1085.

[7] Broomé M, et al. Closed-loop real-time simulation model of hemodynamics and oxygen transport in the cardiovascular system. Biomed Eng Online 2013;12(1):69.

[8] Sološenko A, et al. Modeling of the photoplethysmogram during atrial fibrillation. Comput Biol Med 2017;81:130–138.

[9] Guerrero G. Analyse à base de modèles des interactions cardiorespiratoires chez l'adulte et chez le nouveau-né. Ph.D. thesis, Université de Rennes 1, LTSI - INSERM U1099, 2020.

[10] Guerrero G, et al. Modeling Patient-Specific Desaturation Patterns in Sleep Apnea. IEEE Trans Biomed Eng 2022; 69(4):1502–1511.

[11] Hernández AI, et al. Model-based interpretation of cardiac beats by evolutionary algorithms: signal and model interaction. Artif Intell Med 2002;26(3):211–235.

[12] Ojeda D, et al. Towards an atrio-ventricular delay optimization assessed by a computer model for cardiac resynchronization therapy. In IX International Seminar on Medical Information Processing and Analysis, volume 8922. 2013; 333–336.

[13] Stergiopulos N, et al. Determinants of stroke volume and systolic and diastolic aortic pressure. Am J Physiol Heart Circ Physiol 1996;270(6):H2050–H2059.

[14] Le Rolle V, et al. Mathematical Modeling of Respiratory System Mechanics in the Newborn Lamb. Acta Biotheor 2013;61(1):91–107.

[15] Morris M. Factorial Sampling Plans for Preliminary Computational Experiments. Technometrics 1991;33(2):161–174.

[16] Hall JE, Hall ME. Guyton and hall textbook of medical physiology. 14 edition. Elsevier, 2020. ISBN 978-0-323-59712-8.

[17] Villegas-Martinez M, et al. Pulse arrival time variation as a non-invasive marker of acute response to cardiac resynchronization therapy. EP Europace 2023;25(3):1183–1192.

Address for correspondence:

Virginie Le Rolle
Université de Rennes, LTSI, Rennes, 35042, France
virginie.lerolle@univ-rennes.fr